EFFECT OF SOLVENTS ON POROUS PROPERTIES OF MICROPOROUS POLYPHENYLENES

Cite this: *INEOS OPEN*, **2024**, *7 (4–5)*, 149–153
DOI: 10.32931/io2447a

Received 8 June 2024,
Accepted 17 July 2024

http://ineosopen.org

S. A. Sorokina,*[a] N. V. Kuchkina,[a] T. D. Patsaev,[b] and Z. B. Shifrina[a]

[a] *Nesmeyanov Institute of Organoelement Compounds, Russian Academy of Sciences, ul. Vavilova 28, str. 1, Moscow, 119334 Russia*
[b] *National Research Centre "Kurchatov Institute", pl. Akademika Kurchatova 1, Moscow, 123182 Russia*

Abstract

Microporous organic polymers are of considerable interest for the development of gas separation technologies, catalysis, gas storage systems and other areas. This study shows the effect of porogenic solvents (toluene, *o*-xylene, DMF) on the pore size distribution, volume and content of micropores in microporous polyphenylenes. Using scanning electron microscopy, a strong effect of solvents on the morphology of the resulting polymers was shown. The nitrogen adsorption–desorption isotherms allowed for determining the optimal conditions for the synthesis of soluble microporous polyphenylenes, leading to samples with the highest degree of microporosity.

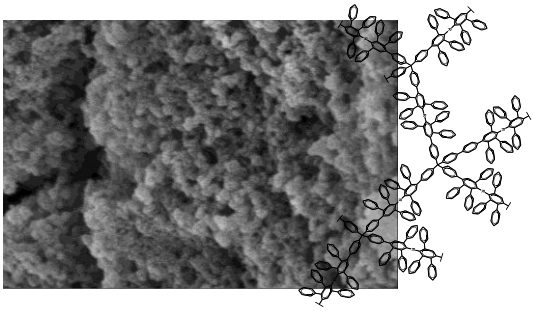

Key words: porous properties, surface area, porogen, microporous polymers, polyphenylenes.

Introduction

Porous organic polymers (POPs) are of particular interest for the development of new technologies for the chemical industry and are attractive from both practical and theoretical points of view. The development of the chemistry of porous organic compounds in the last two decades has led to the emergence of new gas separation technologies and gas storage systems and has contributed to progress in catalytic technologies [1–4]. The main classes of microporous compounds include porous aromatic frameworks (PAFs) [5], microporous conjugated polymers (CMPs) [6, 7], covalent triazine frameworks (CTFs) [8, 9], hypercrosslinked polymer networks [10, 11], metal-organic frameworks (MOFs) [12, 13], and structurally related covalent-organic frameworks (COFs) [14, 15], obtained using reversible reactions of covalent bond formation. Of note are also soluble microporous polymers, including polymers with internal microporosity, the main advantage of which is the possibility of direct processing from solution [16, 17]. At the same time, despite the development of new and improvement of old approaches to the synthesis of microporous polymers, one of the key problems remains the heterogeneity of pores, as well as the complexity of controlling the size and volume of pores, the proportion of micropores in the total surface area during synthesis. Obviously, these parameters are significantly affected by both the structure of the monomers and the selected synthetic method, as well as the reaction conditions.

The strong influence of the reaction conditions, primarily the solvent, on the porosity of polymers has been known for a long time. For example, the porous properties of methacrylate polymers can change significantly under the action of the so-called porogenic solvents, for which ethanol and methanol were studied [18]. In general, an increase in the concentration of the porogenic solvent leads to an increase in both the surface area and the pore sizes. In this case, the pore sizes depend on the solubility of the monomers in the initial solvent mixture and the evaporation rate of the porogenic solvent. A similar effect was observed for polycaprolactone films [19]. It was shown that the solvent strongly affects the porous properties of polyimide aerogels [20]. In this case, the variation of the solvent and the composition of the solvent mixture allowed for tuning the specific surface area, sizes and morphology of pores.

It should be noted that, among microporous polymers, a systematic study of the effect of a solvent on the porous properties has been carried out only for CMPs. Thus, Mollart and Trewin [21] found that the porosity parameters strongly depend on the solvent polarity, the interaction between the solvent and monomers, including the formation of hydrogen bonds, as well as the phase separation between the formed polymer and solvent. Recently, the same research group showed that the use of DMF for the synthesis of CMPs allows one to obtain a polymer with the highest proportion of micropores, while the polymer obtained in THF is characterized by a similar surface area, most of which, however, falls on the mesopores [22]. In addition, a number of studies have demonstrated that the addition of inorganic salts to the reaction mixture during the synthesis of CMPs enables the optimization of the surface area and pore size distribution without changing the chemical composition of the polymer owing to a change in the Hansen solubility parameters [23, 24].

Of note is also that the synthesis of microporous polymers, in which the main part of the surface area falls just on micropores, is one of the key problems of the chemistry of microporous polymers. In general, the developed surface area of

porous organic polymers falls on both micro and mesopores. However, it is due to the presence of micropores that porous polymers exhibit their special properties, which allow them to be used for gas storage and separation systems, as well as for the formation of selective catalysts. In this respect, the development of methods for varying surface properties, namely, specific area, sizes and size distribution of pores, the content of micropores in the total porosity value is extremely important for obtaining materials with better performance characteristics.

Recently, we have synthesized microporous polyphenylenes (PPs) using the Diels–Alder polycondensation of multifunctional ethynyl-containing monomers of different spatial architecture with bis(cyclopentadienones) [25]. The resulting polymers were soluble in organic solvents, and their specific surface area reached 751 m^2/g. We showed that the variation of the monomer structure can effectively change the pore sizes of the resulting polymer and its surface area. The surface area, in turn, also depended on the molecular weight of the polymer. However, the effect of the solvent on the porous properties was not taken into account in the work. All experiments were carried out in diphenyl ether, which is a good solvent for both the initial monomers and the polymer. In this work, we demonstrate the possibility of varying the surface properties of soluble microporous polyphenylenes, developed by us earlier, using porogenic solvents, such as toluene, *o*-xylene, and DMF.

Results and discussion

The synthesis of microporous soluble PPs was carried out by the Diels–Alder reaction, according to the principles developed by us earlier. In order to prevent the formation of a cross-linked structure, the reaction was carried out in a dilute solution at an equifunctional ratio of monomers (A4:B2 = 1:2). The synthetic scheme is shown in Fig. S1 in the Electronic supplementary information (ESI). Tetrakis(4-ethynylphenyl)methane (A4) and 3,3'-(1,4-phenylene)bis(2,4,5-triphenylcyclopenta-2,4-dien-1-one (B2) were used as monomers. Earlier we have shown that the use of a tetrahedral monomer, tetrakis(4-ethynylphenyl)methane, as an ethynyl-containing monomer leads to the production of microporous polyphenylenes with a developed surface area (S_{BET} = 667 m^2/g) and pore sizes of 0.6–1.0 nm, whereas the use of the mentioned bis(cyclopentadienone) is more preferable for the synthesis of microporous PP. To study the possibility of variation of the surface properties depending on a solvent, several porogenic solvents, namely, toluene, *o*-xylene, and DMF were added to the main solvent during the polycondensation. These solvents affect the porous properties of the resulting polymer due to: (1) changing the reaction temperature and (2) the formation of bubbles on the surface of polymer particles due to active boiling of the solvent. While the formation of bubbles affects the morphology of the formed polymers, a decrease in the temperature undoubtedly affects the reaction kinetics and, along with this, reduces the molecular weight of the products. Taking into account that the previously developed PPs based on tetraphenylmethane were characterized by low molecular weights (16.3–47.4 kDa), diphenyl ether, which was used as a solvent earlier, was replaced for dichlorobenzene. Indeed, the use of dichlorobenzene instead of diphenyl ether provided a significant increase in the PP molecular weight up to 345.9 kDa. The experimental results are presented in Table 1.

Table 1. Resulting polyphenylenes and their molecular-weight characteristics

Exp.[a]	Solvent	M_w, kDa[b]	M_w/M_n	Yield, %
1	dichlorobenzene	345.9	18.5	98.0
2	dichlorobenzene–toluene	161	11.5	90.5
3	dichlorobenzene–*o*-xylene	65	1.9	88.5
4	dichlorobenzene–DMF	190	10.1	95.5

[a] reaction conditions: A4:B2 = 1:2, total molar concentration of monomers 0.01 mol/L, synthesis time 8 h;
[b] molecular weight was measured by gel permeation chromatography using the polystyrene standards.

As can be seen from the data in Table 1, the addition of the porogenic solvent resulted in a decrease in the molecular weight: 161 kDa for toluene and 190 kDa for DMF. Interestingly, the greatest decrease in the molecular weight was observed for *o*-xylene: 65 kDa. At the same time, the polydispersity index decreased with the addition of the porogenic solvents. All the polymers were obtained in good yields and represented light beige powders soluble in common organic solvents (chlorinated hydrocarbons, benzene, toluene, and THF).

The surface properties of the resulting polymers were studied using nitrogen adsorption–desorption measurements at 77 K (Fig. 1). Based on the results obtained, the specific surface area and pore volume were calculated (Table 2).

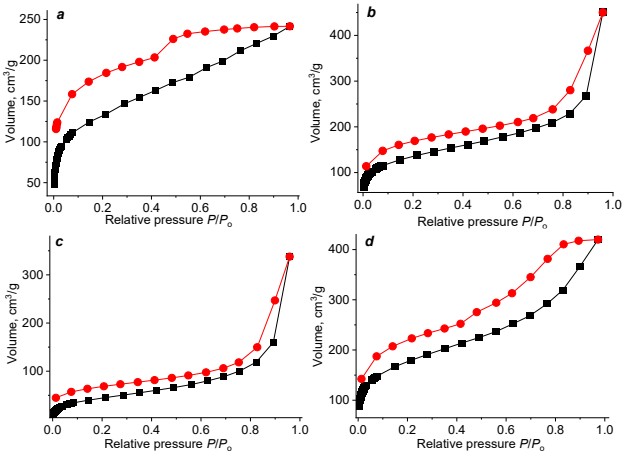

Figure 1. Nitrogen adsorption–desorption isotherms at 77 K for microporous polyphenylenes: 1 (***a***), 2 (***b***), 3 (***c***), 4 (***d***).

All the resulting isotherms demonstrate a sharp rise of the curve in the region of low relative pressures, which indicates the microporous nature of the samples. An increase in the relative pressure leads to the appearance of a hysteresis loop, which implies the presence of a mesoporous structure. The appearance of the curves is typical for microporous polymers [26].

The surface characteristics calculated based on the nitrogen adsorption–desorption isotherms are presented in Table 2. The BET and t-plots are presented in Figs. S3–S6 in the ESI. All the resulting polymers are characterized by the high surface area ranging within 481–640 m^2/g. The exception was sample 3,

obtained in the presence of *o*-xylene, the surface area of which was 287 m^2/g. The addition of toluene and DMF (PPs 2 and 4) ensured an increase in the content of micropores in the total surface area compared to the polymer obtained in pure dichlorobenzene (PP 1). While the proportion of micropores in PP 1 is 32%, for compounds 2 and 4 their proportion increased to 51 and 53%, respectively. Moreover, the addition of porogenic solvents also increased the total pore volume and micropore volume. The best results were obtained for sample 4, synthesized with the addition of DMF. It is characterized by the largest surface area (640 m^2/g), half of which is comprised by micropores, and the largest micropore volume. Thus, the addition of toluene and DMF not only increases the specific surface area, but also significantly improves the microporous characteristics of polyphenylenes.

Table 2. Surface characteristics of microporous polyphenylenes

Sample	S_{BET},[a] $m^2 \cdot g^{-1}$	S_{micro},[b] $m^2 \cdot g^{-1}$	S_{micro}/S_{BET}, %	V_{total},[c] $cm^3 \cdot g^{-1}$	V_{micro},[d] $cm^3 \cdot g^{-1}$
1	481	155	32.2	0.374	0.070
2	490	252	51.4	0.697	0.099
3	287	95	33.1	0.523	0.062
4	640	343	53.6	0.650	0.116

[a] surface area calculated by the BET method;
[b] micropore surface area calculated by the t-plot method;
[c] total volume of pores calculated at $P/P_0 = 0.99$;
[d] volume of micropores calculated by the t-plot method.

The pore size distribution was analyzed using the NLDFT method. The plots are shown in Fig. 2. PP 1 obtained in dichlorobenzene is characterized by a bimodal pore size distribution with the main peak located at 1.3 nm and an insignificant peak at 3.6 nm (Fig. 2a). The addition of DMF (Fig. 2d) did not affect the nature of the pore size distribution. However, the use of toluene and *o*-xylene led to the broadening of the peak related to the mesoporous range. Thus, the addition of toluene not only increases the proportion of micropores in the sample, but also leads to an increase in the mesopore sizes. However, according to the data in Table 1, the appearance of new pores in 4–8 nm region does not affect the microporous nature of the sample, since most of the surface is accounted for micropores.

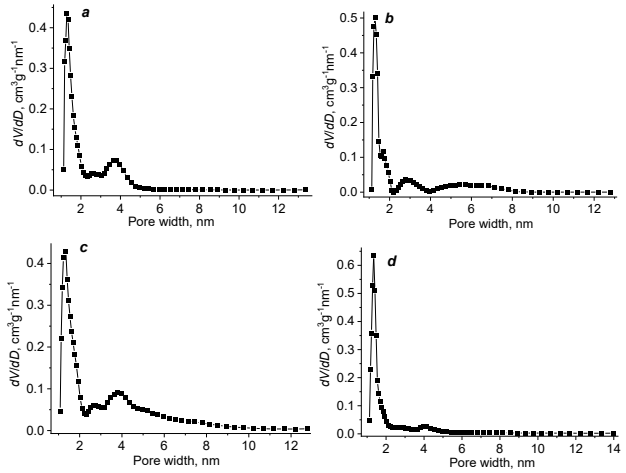

Figure 2. Pore size distributions calculated by NLDFT method for PP samples: 1 (***a***), 2 (***b***), 3 (***c***), 4 (***d***).

The morphology of the resulting polyphenylenes was studied by SEM. Figure 3 clearly shows the change in the PP morphology upon addition of the porogenic solvents. Thus, PP 1 (Fig. 3a) is characterized by the dense packing of particles. The same picture is observed in the case of PP 3 (Fig. 3c), obtained upon addition of *o*-xylene; this sample was characterized by the smallest surface area. However, PPs 2 and 4, obtained using toluene and DMF (Figs. 3b and 3d, respectively), have a spongy morphology. The most expressed porous structure was detected for sample 2, which, however, may be associated with the active formation of bubbles on the surface of the particles due to the strong boiling of toluene, which prevents their aggregation, as well as the appearance of new pores in the mesoporous range.

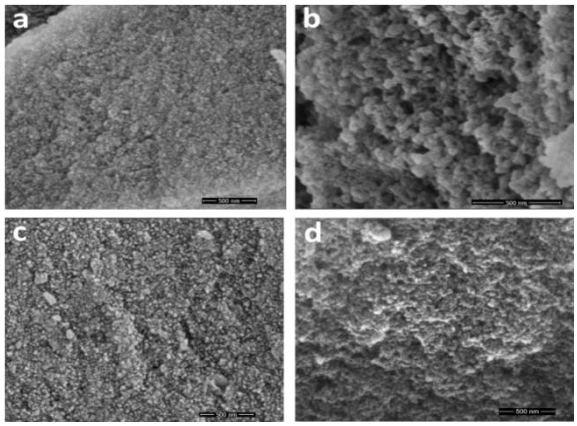

Figure 3. SEM micrographs obtained for PP samples: 1 (***a***), 2 (***b***), 3 (***c***), 4 (***d***).

It is noteworthy that the presence of a certain amount of mesopores, along with micropores, is favorable for the use of microporous polymers in catalytic technologies. Thus, Huang *et al.* [27] showed that the catalytic system based on a metal-organic framework consisting entirely of micropores had lower catalytic activity compared to the system containing both micro- and mesopores, which was associated with deterioration of the substrate/product transport and a decrease in the reaction kinetics. Thus, the catalytic activity of the systems based on microporous polymers is determined by a number of factors: 1) a developed surface area, ensuring the availability of active centers; 2) the presence of mesopores, facilitating the diffusion of molecules. In this regard, the formation of a structure with large pore sizes, observed in the case of toluene, may be attractive for the creation of catalytic systems, and the use of DMF, which leads to the production of soluble polyphenylenes with high molecular weights, a narrow size distribution and a large proportion of micropores, is promising for the synthesis of polymers processed from solution into gas separation membranes.

Experimental section

Materials

Tetraphenylmethane (95%, ABCR), bromine (99%, Acros Organics), trimethylsilylacetylene (98%, ABCR), copper(I) bromide (98%, Sigma-Aldrich), tetrakis(triphenylphosphine)palladium(0) (99%, Sigma-Aldrich), tetrabutylammonium fluoride (1M solution in THF, ABCR),

1,4-diiodobenzene (98%, ABCR), phenylacetylene (98%, Acros Organics), 1,3-diphenyl-2-propanone (99%, Sigma-Aldrich), potassium hydroxide (99%, Acros Organics), glacial acetic acid (99%, Sigma-Aldrich), potassium permanganate, triethylamine (99%, Acros Organics), toluene (99.5%, Komponent Reaktiv), *o*-xylene (99.5%, Komponent Reaktiv), dry DMF (99.8%, Acros Organics), ethanol (96%, Komponent Reaktiv), dichlorobenzene (99%, ABCR), THF (HPLC grade, Carlo Erba reagents), N_2 (99.999%) were purchased from commercial sources.

Synthesis of the microporous polyphenylenes

The polyphenylenes were obtained according to the procedure described in Ref. [25]. The synthetic scheme is presented in Fig. S1 in the ESI. The synthesis was carried out by the polycondensation by the Diels–Alder reaction between tetrakis(4-ethynylphenyl)methane and bis(cyclopentadienone) containing two diene groups. Before the beginning, the reaction mixture was deoxygenated—filled with argon. The total molar concentration of the monomers was 0.01 mol/L; the synthesis was carried out for 8 h. The porogen solvent was used in a 1:1 ratio with dichlorobenzene, while the total concentration of the monomers remained unchanged. The polymers were isolated by repeated reprecipitation in hot ethanol, after which the powder was dried in a vacuum oven at 50 °C.

Characterization

The molecular weights of the polymers were determined by gel permeation chromatography using a Shimadzu LC-20AT chromatograph equipped with two PSS SDV 100 Å and 100000 Å analytical columns installed consecutively and a refractive index detector. THF was used as an eluent, and the analysis was carried out at a flow rate of 1 mL/min. The molecular weights were calculated using the Shimadzu Lab Solutions software relative to polystyrene standards.

The surface area and pore size distribution were measured by nitrogen adsorption–desorption at 77 K using a Quantochrome Nova 1200e analyzer. Prior to the measurements, the sample was dried under vacuum at 60 °C for 24 h. The surface area was calculated using the Brunauer–Emmett–Teller (BET) equation according to the Rouquerol criteria. The cross-sectional area of N_2 and the density of adsorbed N_2 were taken to be 0.162 nm^2 and 0.808 g/mL, respectively. The proportion of micropores was calculated using the t-plot method. The pore size distribution and pore volumes were obtained by the NLDFT method.

Scanning electron microscopy was performed using a Helios Nanolab 600 scanning electron microscope (SEM) (ThermoFisher Scientific, USA). The surface images were obtained using an ETD (Everhardt–Thornley Detector) secondary electron detector in different modes depending on the sample surface charging at an accelerating voltage of 10 kV and a current of 0.17 nA, 5 kV, and 43 pA. Before analysis, the samples were sputtered with a gold layer in an SPI coater (SPI, USA).

Conclusions

The present study provides the simple method for varying the surface properties of soluble microporous polymers by using porogenic solvents during the synthesis. It was shown that the surface area, morphology, number of micropores, and pore size distribution of microporous polyphenylenes varied depending on the porogenic solvent in use. The addition of DMF and toluene significantly improved the microporous properties of polyphenylenes by increasing the proportion of micropores to 50%. The highest value of the surface area, volume, and proportion of micropores was achieved using DMF. The use of the lower boiling porogenic solvent, namely, toluene, along with an increase in the number of micropores also led to an increase in the mesopore sizes. The study opens up new possibilities for controlling and optimizing the surface properties by selecting the most suitable solvent/porogenic solvent pair and can be used for the synthesis of microporous polymers with the given properties.

Acknowledgements

This work was supported by the Russian Science Foundation (project no. 22-73-00087).

Corresponding author

* E-mail: sorokinas@ineos.ac.ru. Tel: +7(499)135-9355 (S. A. Sorokina)

Electronic supplementary information

Electronic supplementary information (ESI) available online: a general scheme for the synthesis of microporous polyphenylenes, the GPC curves, the BET- and t-plots. For ESI, see DOI: 10.32931/io2447a.

References

1. T. Liu, G. Liu, *Nat. Commun.*, **2020**, *11*, 4984. DOI: 10.1038/s41467-020-15911-8
2. M. G. Mohamed, A. F. M. El-Mahdy, M. G. Kotp, S.-W. Kuo, *Mater. Adv.*, **2022**, *3*, 707–733. DOI: 10.1039/D1MA00771H
3. T. Zhang, G. Xing, W. Chen, L. Chen, *Mater. Chem. Front.*, **2020**, *4*, 332–353. DOI: 10.1039/C9QM00633H
4. W. Song, Y. Zhang, C. H. Tran, H. K. Choi, D.-G. Yu, I. Kim, *Prog. Polym. Sci.*, **2023**, *142*, 101691. DOI: 10.1016/j.progpolymsci.2023.101691
5. Y. Tian, G. Zhu, *Chem. Rev.*, **2020**, *120*, 8934–8986. DOI: 10.1021/acs.chemrev.9b00687
6. J.-S. M. Lee, A. I. Cooper, *Chem. Rev.*, **2020**, *120*, 2171–2214. DOI: 10.1021/acs.chemrev.9b00399
7. W. Zhang, H. Zuo, Z. Cheng, Y. Shi, Z. Guo, N. Meng, A. Thomas, Y. Liao, *Adv. Mater.*, **2022**, *34*, 2104952. DOI: 10.1002/adma.202104952
8. L. Liao, M. Li, Y. Yin, J. Chen, Q. Zhong, R. Du, S. Liu, Y. He, W. Fu, F. Zeng, *ACS Omega*, **2023**, *8*, 4527–4542. DOI: 10.1021/acsomega.2c06961
9. M. Liu, L. Guo, S. Jin, B. Tan, *J. Mater. Chem. A*, **2019**, *7*, 5153–5172. DOI: 10.1039/C8TA12442F
10. L. Tan, B. Tan, *Chem. Soc. Rev.*, **2017**, *46*, 3322–3356. DOI: 10.1039/C6CS00851H
11. Y. Luo, Y. Mei, Y. Xu, K. Huang, *Nanomaterials*, **2023**, *13*, 2514. DOI: 10.3390/nano13182514
12. M. Safaei, M.M. Foroughi, N. Ebrahimpoor, S. Jahani, A. Omidi, M. Khatami, *TrAC, Trends Anal. Chem.*, **2019**, *118*, 401–425. DOI: 10.1016/j.trac.2019.06.007

13. Y. Li, G. Wen, J. Li, Q. Li, H. Zhang, B. Tao, J. Zhang, *Chem. Commun.*, **2022**, *58*, 11488–11506. DOI: 10.1039/D2CC04190A
14. K. Geng, T. He, R. Liu, S. Dalapati, K.T. Tan, Z. Li, S. Tao, Y. Gong, Q. Jiang, D. Jiang, *Chem. Rev.*, **2020**, *120*, 8814–8933. DOI: 10.1021/acs.chemrev.9b00550
15. J. Á. Martín-Illán, D. Rodríguez-San-Miguel, F. Zamora, *Coord. Chem. Rev.*, **2023**, *495*, 215342. DOI: 10.1016/j.ccr.2023.215342
16. N. B. McKeown, *Polymer*, **2020**, *202*, 122736, DOI: 10.1016/j.polymer.2020.122736
17. F. Topuz, M. H. Abdellah, P. M. Budd, M. A. Abdulhamid, *Polym. Rev.*, **2024**, *64*, 251–305. DOI: 10.1080/15583724.2023.2236677
18. S. Yu, F. L. Ng, K. C. C. Ma, A. A. Mon, F. L. Ng, Y. Y. Ng, *J. Appl. Polym. Sci.*, **2013**, *127*, 2641–2647. DOI: 10.1002/app.37514
19. F. Safaei, S. Khalili, S. Nouri Khorasani, L. Ghasemi-Mobarakeh, R. Esmaeely Neisiany, *J. Polym. Sci. Eng*., **2018**, *1* 1076. DOI: 10.24294/jpse.v1i4.1076
20. D. H. Lee, M. J. Jo, S. W. Han, S. Yu, H. Park, *Polymer*, **2020**, *205*, 122879. DOI: 10.1016/j.polymer.2020.122879
21. C. Mollart, A. Trewin, *Phys. Chem. Chem. Phys.*, **2020**, *22*, 21642–21645. DOI: 10.1039/D0CP03539D
22. C. Mollart, A. Trewin, *J. Mater. Chem. A*, **2024**, *12*, 4159–4168. DOI: 10.1039/D3TA04866G
23. J. Chen, W. Yan, E. J. Townsend, J. Feng, L. Pan, V. Del Angel Hernandez, C. F. J. Faul, *Angew. Chem*., *Int. Ed.*, **2019**, *58*, 11715–11719. DOI: 10.1002/anie.201905488
24. J. Chen, T. Qiu, W. Yan, C. F. J. Faul, *J. Mater. Chem. A*, **2020**, *8*, 22657–22665. DOI: 10.1039/D0TA05563H
25. S. A. Sorokina, N. V. Kuchkina, A. V. Mikhalchenko, I. Y. Krasnova, D. A. Khanin, K. M. Skupov, Z. B. Shifrina, *Polymers*, **2023**, *15*, 2060. DOI: 10.3390/polym15092060
26. M. Minelli, D. R. Paul, G. C. Sarti, *J. Membr. Sci.*, **2017**, *540*, 229–242. DOI: 10.1016/j.memsci.2017.06.053
27. G. Huang, L. Yang, X. Ma, J. Jiang, S.-H. Yu, H.-L. Jiang, *Chem. Eur. J.*, **2016**, *22*, 3470–3477. DOI: 10.1002/chem.201504867